Kosambi-Cartan-Chern perspective on chaos: Unveiling hidden attractors in nonlinear autonomous systems

Somnath Roy [*]
Department of Physics, Jadavpur University, Kolkata 700075, India

Anirban Ray [†]
Department of Physics, Gour Mahavidyalaya, Mangalbari, Malda 732142, India

A. Roy Chowdhury [‡]
Department of Physics, Jadavpur University, Kolkata 700075, India

(Received 27 November 2023; accepted 20 March 2024; published 8 April 2024)

This article confronts the formidable task of exploring chaos within hidden attractors in nonlinear three-dimensional autonomous systems, highlighting the lack of established analytical and numerical methodologies for such investigations. As the basin of attraction does not touch the unstable manifold, there are no straightforward numerical processes to detect those attractors and one has to implement special numerical and analytical strategies. In this article we present an alternative approach that allows us to predict the basin of attraction associated with hidden attractors, overcoming the existing limitations. The method discussed here is based on the Kosambi-Cartan-Chern theory which enables us to conduct a comprehensive theoretical analysis by means of evaluating geometric invariants and instability exponents, thereby delineating the regions encompassing chaotic and periodic zones. Our analytical predictions are thoroughly validated by numerical results.

DOI: 10.1103/PhysRevE.109.044205

I. INTRODUCTION

From the latter half of the century onwards, the enigmatic world of chaotic oscillators has beckoned researchers, casting a spell of fascination and intrigue that continues to deepen. In that period, chaotic self-excited attractors were found numerically [1,2] by standard numerical procedure, in which the trajectory starting from an unstable manifold in the vicinity of equilibrium reaches a state of oscillation after an intermediate transient process; thereby localization of the basin of attraction of these kinds of self-excited chaotic oscillators is somewhat systematic. Since that time, an abundance of research has been diligently carried out in this fascinating realm [3–13]. In recent times, a significant surge of scholarly attention has been directed towards a remarkable development, spurred by the seminal work of Kuznetsov, Lenov, and Vagaitsev [14]. This notable advancement unveils a distinctive class of attractors, characterized as *hidden attractors* [15–19], where the basin of attraction remains devoid of any intersection with the unstable manifold of equilibrium points. For instance, within the framework of dynamical systems, cases characterized by the absence of any equilibrium points or the existence of only a single equilibrium point engender the emergence of chaotic hidden oscillations [20–26]. In such intricate scenarios, the computational and analytical endeavor associated with the localization of the basin of attraction assumes a distinctly formidable character, primarily due to the inherent challenge posed by the unavailability of *a priori* equilibrium point information. Extensive research efforts in recent years have been directed towards the localization of hidden attractors, employing both numerical and analytical approaches. Numerical procedures encompass methodologies such as homotopy and continuation techniques [27], while analytical methods are rooted in the construction of Lyapunov functions and an assessment of the dissipative properties inherent to the system [28]. Additionally, a novel approach has emerged involving the construction of perpetual points [29].

However, despite these significant advancements, the field currently lacks an analytical method capable of predicting the basin of attraction for hidden oscillators. Addressing this critical gap in the existing body of knowledge constitutes the central focus of our article. In our pursuit, we employ a geometrodynamical approach, rooted in the Kosambi-Cartan-Chern (KCC) theory [30–32], which is founded on the principles of Finsler space theory [33,34]. This approach holds the promise of shedding new light on the intricate problem of predicting the basin of attraction for hidden oscillators.

While global stability analysis of chaotic systems can traditionally be characterized through Lyapunov stability assessments, it is worth noting that the numerical calculation of Lyapunov exponents, often necessitating substantial computational resources, can pose considerable challenges in practice. A commonly utilized and highly effective numerical approach for computing the Lyapunov spectrum in a smooth dynamical system is through periodic Gram-Schmidt orthonormalization of the Lyapunov vectors. This method is employed to prevent the misalignment of all vectors along the direction of maximal

[*]roysomnath63@gmail.com
[†]anirban.chaos@gmail.com
[‡]Corresponding author: arc.roy@gmail.com

 ©2024 American Physical Society

expansion. While this method is extensively used, achieving better accuracy often necessitates running a large number of iterations, which can be both time-consuming and computationally challenging.

Alternatively, within the framework of the KCC theory, one finds a compelling avenue for stability analysis. Among the five geometric invariants offered by the KCC theory, the second invariant, namely, the *deviation curvature tensor* (P^i_j), provides a valuable insight into the bunching and dispersing behavior of nearby trajectories, near the arbitrarily chosen initial positions. This approach offers an alternative perspective on stability analysis, commonly known as Jacobian stability. Jacobi stability analysis, as elucidated in detail by Harko *et al.* [35], has become a pivotal tool in the analysis of complex dynamical systems. Its applicability extends across a diverse spectrum of systems, including but not limited to the renowned Lorenz, Rossler, Rabinovich-Fabrikant, and Chen chaotic systems [36–40]. Furthermore, Jacobi stability analysis has found successful application in the study of biological systems, encompassing areas such as cell dynamics [41,42], prey-predator models [43], and competitive models [44]. Its versatility is further underscored by its effectiveness in the investigation of various bifurcation phenomena [45,46], establishing it as an indispensable analytical framework in the realm of nonlinear dynamics.

In this article, we delve into the dynamics of two unique three-dimensional (3D) systems. The first system, characterized by a single stable fixed point [25], presents an intriguing dynamic that captures our attention. Conversely, the second system, devoid of any fixed points [47], represents a rare and complex scenario in dynamical systems. Surprisingly, both systems exhibit hidden chaotic oscillations, adding to their enigmatic nature. Our primary focus is to uncover the underlying dynamics of these systems by exploring the basin of attraction, an area in phase space where trajectories ultimately converge. We aim to achieve this by meticulously analyzing deviation vectors originating from various initial points within the phase space. This approach allows us to gain valuable insights into the intricate dynamics at play, shedding light on the hidden chaotic behavior exhibited by these systems.

II. REVIEW OF KCC THEORY AND JACOBI STABILITY

We revoke the fundamentals of the KCC theory which will be used in the following sections. We follow the work of Böhmer *et al.* [35]. Let $p = (x, y) \in T\mathcal{M}$, where $x = (x^1, x^2, \ldots, x^n)$, $y = (y^1, y^2, \ldots, y^n)$, and $T\mathcal{M}$ is the tangent bundle of the smooth n-dimensional manifold $\mathcal{M} = \mathbb{R}^n$. Now consider an open connected subset $\Omega \in \mathbb{R}^n \times \mathbb{R}^n \times \mathbb{R}$ and $(x, y, t) \in \Omega$, where we consider a system of second-order differential equations in the form of

$$\frac{d^2x^i}{dt^2} + 2G^i(x, y, t) = 0, \qquad i \in \{1, 2, \ldots, n\}, \tag{2.1}$$

where G^i is a smooth function of local coordinates defined on $T\mathcal{M}$. Now by defining the time-independent coordinate transformation $\tilde{x}^i = \tilde{x}^i(x^1, x^2, \ldots, x^n)$ and $\tilde{y}^i = \frac{\partial \tilde{x}^i}{\partial x^j} y^j$, the equivalent vector field V on $T\mathcal{M}$ of Eq. (2.1) is given by

$$V = y^i \frac{\partial}{\partial x^i} - 2G^i(x^j, y^j, t)\frac{\partial}{\partial y^i}, \tag{2.2}$$

from which one can establish the nonlinear connection N^j_i defined by [35]

$$N^j_i = \frac{\partial G^i}{\partial y^j}. \tag{2.3}$$

We can proceed further to obtain the covariant differential of the vector field $\xi^i \subseteq \Omega$ as [35]

$$\frac{D\xi^i}{dt} = \frac{d\xi^i}{dt} + N^i_j \xi^j. \tag{2.4}$$

Substituting $\xi^i = y^i$, we can generate

$$\frac{Dy^i}{dt} = N^i_j y^j - 2G^i = -\epsilon^i, \tag{2.5}$$

where ϵ^i is the contravariant vector field defined on Ω and known as the *first KCC invariant* which physically implicates the external force present in the system.

If we now deviate the trajectory of the system in Eq. (2.1) from nearby ones according to

$$\tilde{x}^i(t) = x^i(t) + \eta\xi^i(t), \tag{2.6}$$

with $\| \eta \|$ treated as a small perturbation parameter and ξ^i as a component of the contravariant vector field along the path x^i, and substitute the above equation into Eq. (2.1) and take the limit $\eta \longrightarrow 0$, we can arrive at the variational equations [35]

$$\frac{d^2\xi^i}{dt^2} + 2N^i_j \frac{d\xi^j}{dt} + 2\frac{\partial G^i}{\partial x^j}\xi^j = 0. \tag{2.7}$$

With the KCC covariant differential, the above equation takes the form

$$\frac{D^2\xi^i}{dt^2} = P^i_j \xi^j, \tag{2.8}$$

where P^i_j is defined as

$$P^i_j = -2\frac{\partial G^i}{\partial x^j} - 2G^l G^i_{jl} + y^l \frac{\partial N^i_j}{\partial x^l} + N^i_l N^l_j + \frac{\partial N^i_j}{\partial t}. \tag{2.9}$$

Equation (2.8) is called the *Jacobi equation* of the second-order differential equation, and P^i_j symbolizes the *second KCC invariant or the deviation curvature tensor*, with the Berwald connection denoted as $G^i_{jl} \equiv \frac{\partial N^i_j}{\partial y^l}$. There are three more KCC invariants [35] which are excluded here due to the motive our article.

Now to analyze the Jacobi stability of the trajectories $x^i = x^i(t)$ of Eq. (2.1) in the vicinity of a point x^i ($t_0 = 0$) in the Euclidean space $(\mathbb{R}^n, \langle ., . \rangle)$, we have to study the behavior of the deviation vector ξ^i, which satisfies the initial conditions $\xi(0) = O$ and $\dot{\xi}(0) = W \neq O$, where O is the null vector in $\mathbb{R}^n$. For arbitrary two vectors $\langle\langle X, Y \rangle\rangle \in \mathbb{R}^n$ we consider an adapted inner product $\langle\langle ., . \rangle\rangle$ of ξ such that $\langle\langle X, Y \rangle\rangle := \frac{1}{\langle W, W \rangle} \cdot \langle X, Y \rangle$.

This enables us to describe the bunching and dispersing tendency of ξ around $t_0 = 0$ as follows: as $t \to 0^+$ if $\|\xi\| < t^2$, then the trajectories are bunching together, and if $\|\xi\| > t^2$ as $t \to 0^+$, the trajectories are dispersing.

Definition. If Eq. (2.1) satisfies the initial conditions mentioned above, then the trajectories $x^i(t)$ are called *Jacobi stable* if and only if the real part of the eigenvalues of the deviation curvature tensor $P^i_j(0)$ is negative.

In the upcoming sections, we undertake the analysis of two distinct systems, each exemplifying a unique dynamical characteristic—one with a single equilibrium point and the other devoid of any fixed points. Our objective is to demonstrate that the KCC analysis is adept at extracting the basin of attraction for both systems through an analytical framework. This framework is expressed in terms of a set of coupled differential equations governing the deviation vectors, denoted as ξ^i. By determining the solution of ξ^i, we subsequently define the instability exponent δ_i, akin to the Lyapunov exponent, as a quantitative measure of the chaotic behavior. The deviation vector can be evaluated from its components by

$$\xi(t) = \frac{\sqrt{[\xi^1(t)]^2 + [\xi^2(t)]^2}}{\sqrt{[\dot{\xi}^1(0)]^2 + [\dot{\xi}^2(0)]^2}}. \tag{2.10}$$

Now the instability exponents are defined as

$$\delta_i(x^j, y^j, t) = \lim_{t\to\infty} \frac{1}{t} \ln\left[\frac{\xi^i}{\xi_{i0}}\right], \quad i = 0, 1, \tag{2.11}$$

and

$$\delta(x^j, y^j, t) = \lim_{t\to\infty} \frac{1}{t} \ln\left[\frac{\xi}{\xi_{10}}\right], \tag{2.12}$$

where $\dot{\xi}^1(0) = \xi_{10}$ and $\dot{\xi}^2(0) = \xi_{20}$. It is important to note that the instability exponent, in general, is a function of initial conditions (x^j, y^j, t) and holds the potential to predict the basin. The notable advantage lies in having an analytical description of the instability exponent, in contrast to the Lyapunov exponent, which, in general, defies analytical calculation. In most cases, numerical techniques become imperative for the computation of Lyapunov exponents.

III. STABILITY OF A SYSTEM WITH A SINGLE FIXED POINT

The following system has a single fixed point at $S(x_0, y_0, z_0) = (\frac{1}{4}, \frac{1}{16}, -16a)$:

$$\dot{x} = yz + a, \tag{3.1}$$

$$\dot{y} = x^2 - y, \tag{3.2}$$

$$\dot{z} = 1 - 4x, \tag{3.3}$$

The attractor is shown in Fig. 1. Now we define $x = X^1$, $y = X^2$, and $z = X^3$, and $\dot{x} = Y^1$, $\dot{y} = Y^2$, and $\dot{z} = Y^3$. By rearranging the equations, following the methodology detailed in the previous section, we can express the system as

$$\frac{d^2X^1}{dt^2} + 2G^1 = 0, \tag{3.4}$$

$$\frac{d^2X^2}{dt^2} + 2G^2 = 0, \tag{3.5}$$

where

$$G^1 = \frac{1}{2}\left[X^2(4X^1 - 1) + \frac{Y^2}{X^2}(a - Y^1)\right], \tag{3.6}$$

$$G^2 = \frac{1}{2}[Y^2 - 2X^1Y^1]. \tag{3.7}$$

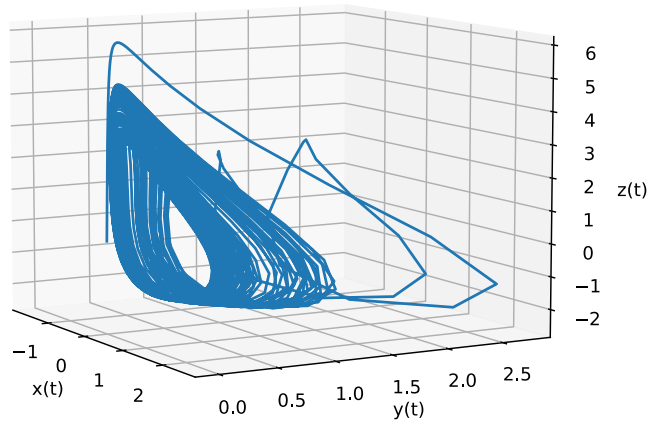

FIG. 1. Attractor of the system of Eqs. (3.1)–(3.3) with the initial condition (0,0,0).

The components of the nonlinear connections are determined by

$$N_1^1 = -\frac{1}{2}\frac{Y^2}{X^2}, \quad N_1^2 = -\frac{1}{2}\frac{a - Y^1}{X^2},$$
$$N_2^1 = -X^1, \quad N_2^2 = \frac{1}{2}. \tag{3.8}$$

The components of the Berwald connection are

$$G_{11}^1 = 0, \quad G_{12}^1 = -\frac{1}{2X^2}, \quad G_{21}^1 = -\frac{1}{2X^2}, \quad G_{22}^1 = 0,$$
$$G_{11}^2 = G_{12}^2 = G_{21}^2 = G_{22}^2 = 0. \tag{3.9}$$

Now by Eq. (2.9), the components of the deviation curvature tensor are expressed as

$$P_1^1 = -4X^2 + \frac{1}{2X^2}[Y^2 - 2X^1Y^1] + \frac{1}{2}\left(\frac{Y^2}{X^2}\right)^2 + \frac{1}{4}\left(\frac{Y^2}{X^2}\right)^2 - \frac{X^1}{2}\left[\frac{a - Y^1}{X^2}\right],$$
$$P_2^1 = \left[\frac{Y^2}{(X^2)^2}(a - Y^1) - (4X^1 - 1)\right] + \frac{1}{2X^2}\left[X^2(4X^1 - 1) + \frac{Y^2}{X^2}(a - Y^1)\right] + \frac{Y^2}{2}\left[\frac{Y^1 - a}{(X^2)^2}\right] - \frac{Y^2}{4(X^2)^2}[a - Y^1] + \frac{1}{4}\left[\frac{a - Y^1}{X^2}\right],$$
$$P_1^2 = Y^1 + \frac{X^1Y^2}{2X^2} - \frac{X^1}{2},$$
$$P_2^2 = \frac{1}{4} - \frac{X^1}{2X^2}(a - Y^1). \tag{3.10}$$

In Fig. 2, the components of P_j^i are depicted with the initial condition set to (0,0,0), while the value of a remains fixed at $a = 0.01$. The plotting of these components is achieved using Eq. (3.10). Now we have all the components of the P_j^i matrix, which can be evaluated at the fixed point $S(x_0, y_0, z_0)$. The

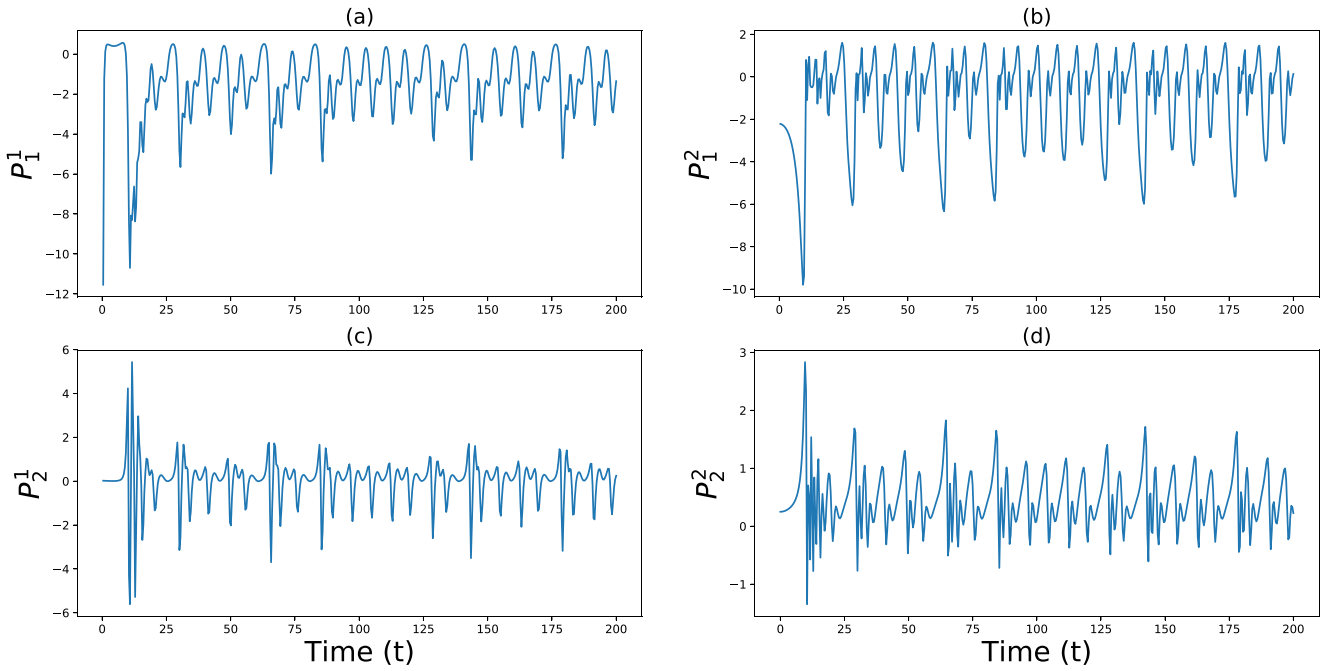

FIG. 2. Components of the deviation curvature tensor P^i_j, Eq. (3.10), as it varies with time for the system of Eqs. (3.1)–(3.3) with the initial condition (0,0,0). (a) $P^1_1\ (t)$ vs time (t). (b) $P^1_2\ (t)$ vs time (t). (c) $P^2_1\ (t)$ vs time (t). (d) $P^2_2\ (t)$ vs time (t).

matrix

$$\begin{bmatrix} P^1_1 & P^2_1 \\ P^1_2 & P^2_2 \end{bmatrix}_S = \begin{bmatrix} -\frac{1}{4} - 2a & 4a \\ -\frac{1}{8} & \frac{1}{4} - 2a \end{bmatrix}$$

gives the characteristics equation

$$\lambda^2 + 4a\lambda + 4a^2 - \frac{1}{16} + \frac{a}{2} = 0. \tag{3.11}$$

The eigenvalues of the above equation are

$$\lambda_{1,2} = -2a \pm \frac{1}{2}\sqrt{\frac{1}{4} - 2a}. \tag{3.12}$$

Clearly the equilibrium $S(x_0, y_0, z_0)$ is Jacobi unstable and it is a saddle focus [35]. The deviation vectors ξ^i can be written by Eq. (2.7) as

$$\frac{d^2\xi^1}{dt^2} - \frac{Y^2}{X^2}\frac{d\xi^1}{dt} + \left(\frac{a - Y^1}{X^2}\right)\frac{d\xi^2}{dt} + 4X^2\xi^1 \left[(4X^1 - 1) - \frac{Y^2}{(X^2)^2}(a - Y^1)\right]\xi^2 = 0 \tag{3.13}$$

and

$$\frac{d\xi^2}{dt} - 2X^1\frac{d\xi^1}{dt} + \frac{d\xi^2}{dt} - 2Y^1\xi^1 = 0. \tag{3.14}$$

Substituting the system's variables in the above equations, we get the forms, respectively, as

$$\frac{d^2\xi^1}{dt^2} - \frac{x^2 - y}{y}\frac{d\xi^1}{dt} - z\frac{d\xi^2}{dt} + 4y\xi^1 \left[(4x - 1) + \frac{z(x^2 - y)}{y}\right]\xi^2 = 0 \tag{3.15}$$

and

$$\frac{d^2\xi^2}{dt^2} - 2x\frac{d\xi^1}{dt} + \frac{d\xi^2}{dt} - 2(yz + a)\xi^1 = 0. \tag{3.16}$$

Equations (3.15) and (3.16) represent a system of coupled differential equations for ξ^1 and ξ^2, offering a depiction of the basin for the system described by Eqs. (3.1)–(3.3). The solutions to these equations can be obtained through numerical methods such as RK-4 or Euler. Subsequently, utilizing Eqs. (2.10) and (2.12), the instability exponent δ can be determined as a function of the system's variables. This approach offers a computationally more tractable alternative to the laborious task of numerically calculating Lyapunov exponents. In Fig. 3, two basins are presented. One is computed by tracing the maximum Lyapunov exponent, while the other is determined by calculating the instability exponent using Eq. (2.12). Remarkably, the figures exhibit a close alignment, providing an accurate visualization of the periodic and chaotic zones associated with the hidden attractor.

Behavior of the deviation vectors near the fixed point

The linear stability analysis reveals the existence of a stable fixed point at S within the system. However, when subjected to Jacobi stability analysis, the equilibrium point emerges as an unstable saddle focus. This intriguing contradiction motivates us to scrutinize the curvature variation around this point. At first Eqs. (3.15) and (3.16) take the form of a linearly coupled equation near the fixed point:

$$\frac{d^2\xi^1}{dt^2} + 16a\frac{d\xi^2}{dt} + \frac{1}{4}\xi^1 = 0 \tag{3.17}$$

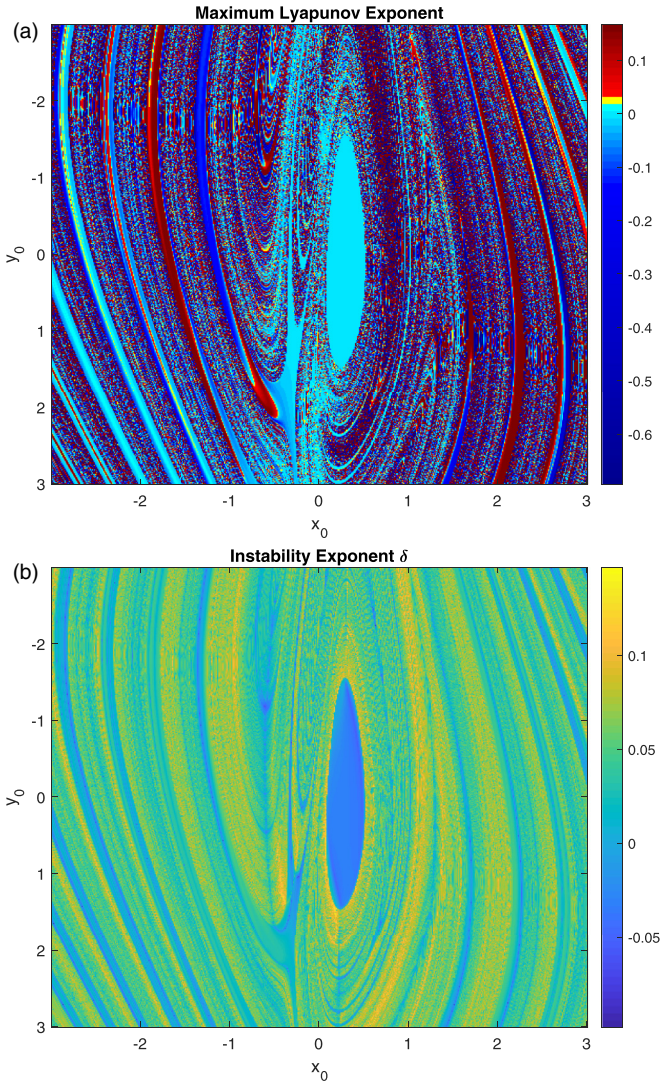

FIG. 3. Basin of attraction of the system Eqs. (3.1)–(3.3). (a) Basin (x_0, y_0) is numerically determined by the estimation of maximum Lyapunov exponent. (b) Basin is determined by calculating the instability exponent δ with the help of the deviation vector computed from Eqs. (3.15) and (3.16).

and

$$\frac{d^2\xi^2}{dt^2} - \frac{1}{2}\frac{d\xi^1}{dt} + \frac{d\xi^2}{dt} = 0. \tag{3.18}$$

From the information of ξ^1 and ξ^2 one can derive the curvature [35] defined as

$$\kappa(S) = \frac{\dot{\xi}^1(t)\ddot{\xi}^2(t) - \dot{\xi}^2(t)\ddot{\xi}^1(t)}{\{[\xi^1(t)]^2 + [\xi^2(t)]^2\}^{\frac{3}{2}}}. \tag{3.19}$$

While ξ^2 and ξ^2 can indeed be analytically computed from the coupled ordinary differential equations provided earlier, and subsequently used to evaluate the curvature κ, we opt to sidestep the cumbersome expression for the sake of brevity. Instead, we numerically solve these elements, allowing us to directly observe their variations. The variation of ξ^1 and ξ^2 is depicted in Fig. 4. Moving beyond the knowledge of deviation vectors, we proceed to illustrate the curvature variation using

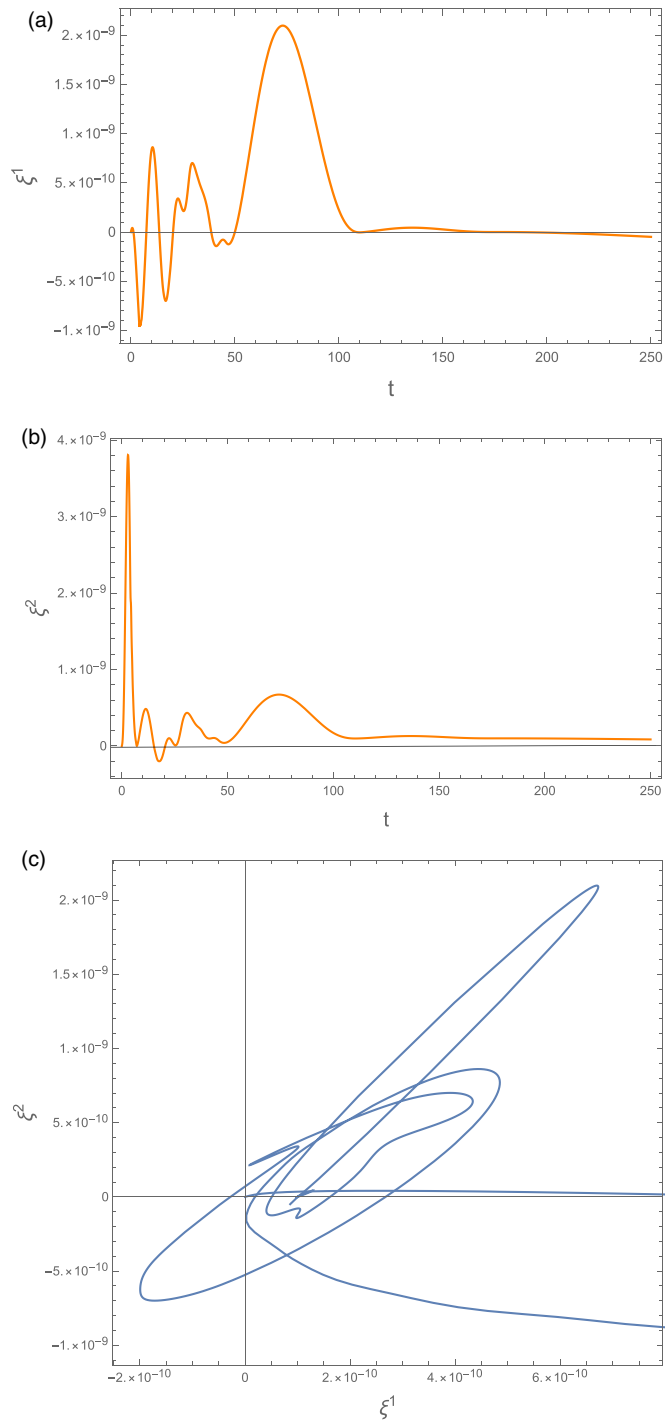

FIG. 4. Deviation vectors are numerically calculated from Eqs. (3.15) and (3.16). (a) Variation of the deviation vector ξ^1 with time. Initial conditions are $\dot{\xi}^1(0) = 10^{-10}$ and $\dot{\xi}^2(0) = 10^{-10}$. (b) Variation of the deviation vector ξ^2 with time. (c) Phase portrait in the ξ^1-ξ^2 plane.

Eq. (3.19) in Fig. 5. It is widely recognized that the onset of chaos within the system can be identified by observing whether the curvature changes sign before a critical minimum time. This critical time, denoted as τ_0, is determined by setting $\xi^1(t_0) = \xi^2(t_0)$, implying the curvature $\kappa(t_0)$ is zero. In Fig. 5(a), the numerical calculation yields a value of approximately 7.5 for τ_0. Furthermore, in Fig. 5(b), it is

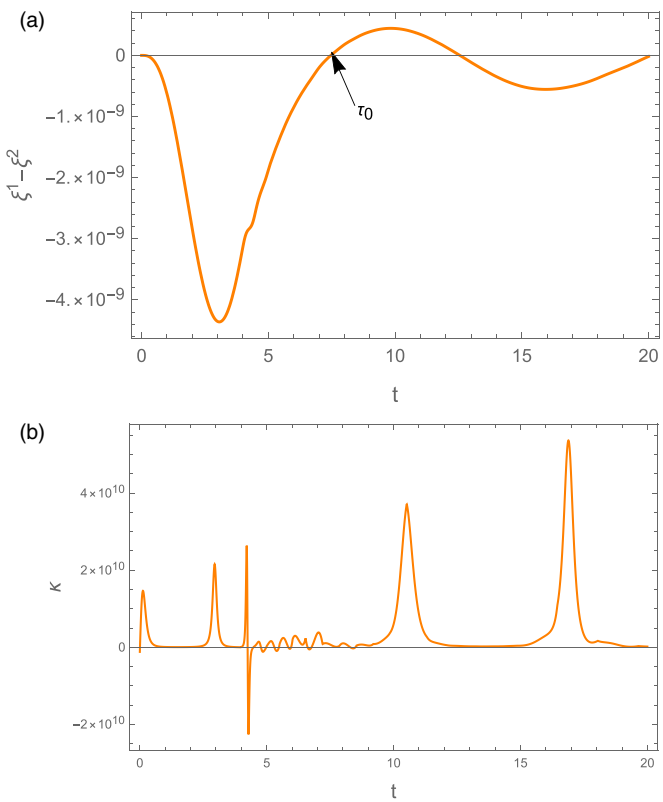

FIG. 5. (a) Critical time τ_0 at which the curvature κ is zero, i.e., $\xi^1(\tau_0) = \xi^2(\tau_0)$, is approximately 7.5. (b) Variation of curvature κ with time (t). It clearly shows that the curvature changes its sign before the critical time, which is a quantitative indication of chaos.

evident that the curvature changes sign before τ_0, indicating that the underlying evolution of this hidden attractor will exhibit chaotic behavior in the long term. The variation of instability exponent δ with time (t) and the variation of deviation vector $\xi(t)$ with t^2 are shown in Figs. 6(a) and 6(b) respectively.

IV. STABILITY OF A SYSTEM WITHOUT A FIXED POINT

Let us consider a system of a Sprott case A hidden attractor [47], which is a special case of a Nose-Hoover [49] system, pertinent to many natural natural phenomenon [48]:

$$\dot{x} = y, \tag{4.1}$$

$$\dot{y} = -x + yz, \tag{4.2}$$

$$\dot{z} = 1 - y^2. \tag{4.3}$$

Despite the inherent conservativity of the system, the absence of any apparent attractor is an expected outcome. However, our investigation uncovers a surprising and fascinating revelation—the presence of a coexisting chaotic sea alongside nested tori, each contingent on varying initial conditions (see Fig. 7). This intriguing phenomenon strongly hints at the existence of a concealed attractor within the system. For the systematic and analytical prediction of the basin of attractor we employ KCC theory as follows.

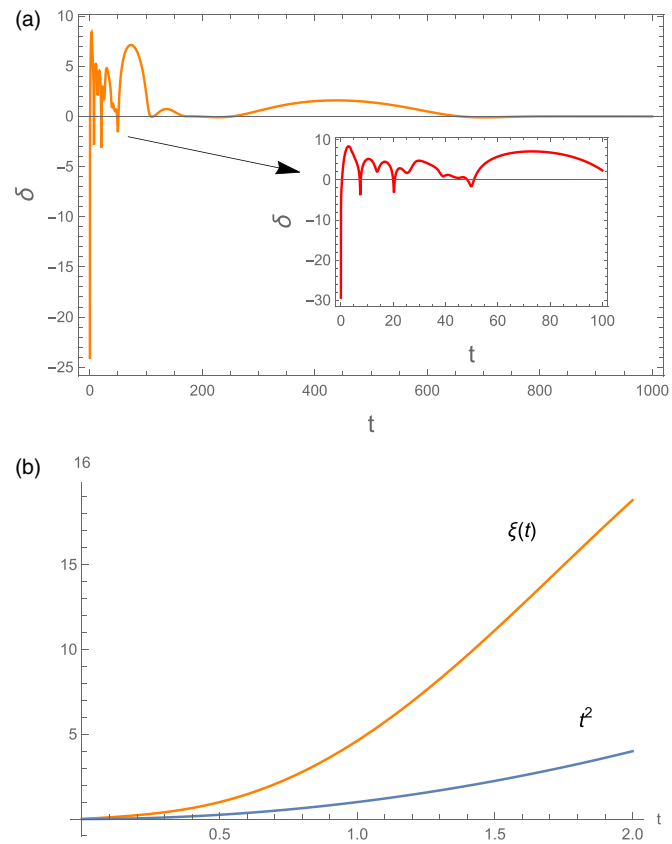

FIG. 6. (a) Instability exponent near the equilibrium point $S(x_0, y_0, z_0)$ for the system of Eqs. (3.1)–(3.3) calculated by Eq. (2.12) and $\xi_{10} = 10^{-10}$. (b) Variation of $\xi(t)$ and t^2 against t.

By Eq. (3.2) taking the derivative on both sides and using $\dot{x} = y$, we arrive at

$$\ddot{y} = -y + \dot{y}z + y\dot{z}. \tag{4.4}$$

Also, Eq. (3.3) gives

$$\ddot{z} = -2y\dot{y}. \tag{4.5}$$

Now express the variables of the system as

$$X^1 = y, \quad X^2 = z, \quad X^3 = x,$$
$$Y^1 = \dot{y}, \quad Y^2 = \dot{z}, \quad Y^3 = \dot{x}, \tag{4.6}$$

and one can symbolize Eqs. (3.4) and (3.5) in comparison with Eq. (2.1) as

$$\frac{d^2X^1}{dt^2} + 2G^1(X^1, X^2, Y^1, Y^2) = 0, \tag{4.7}$$

$$\frac{d^2X^2}{dt^2} + 2G^2(X^1, X^2, Y^1, Y^2) = 0, \tag{4.8}$$

where the expressions for G^i's are specified as

$$G^1 = \tfrac{1}{2}(X^1 - Y^1X^2 - X^1Y^2), \quad G^2 = X^1Y^1. \tag{4.9}$$

Now the coefficients of nonlinear connection, Eq. (2.3), are calculated as

$$N_1^1 = -\tfrac{1}{2}X^2,$$
$$N_1^2 = -\tfrac{1}{2}X^1, \quad N_2^1 = X^1, \quad N_2^2 = 0. \tag{4.10}$$

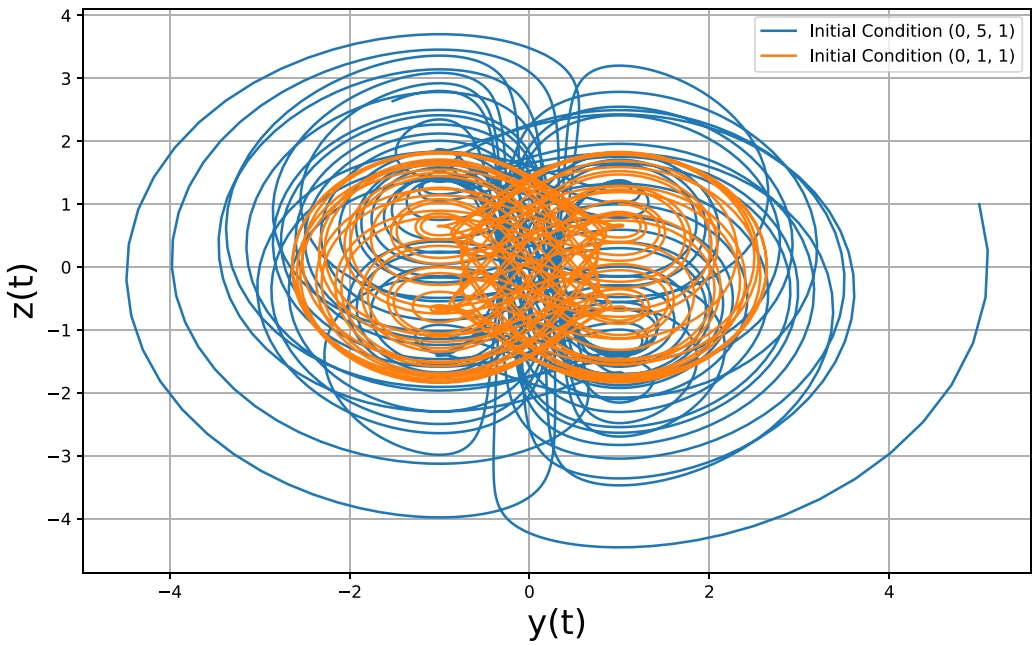

FIG. 7. Phase plot (y-z) of the system of Eqs. (4.1)–(4.3) with two different initial conditions (0,1,1) and (0,5,1).

The components of the Berwald connection $G^i_{jl} = \frac{\partial N^i_j}{\partial Y^l}$ are worked out as

$$G^1_{11} = G^1_{12} = G^1_{21} = G^1_{22} = 0,$$
$$G^2_{11} = G^2_{12} = G^2_{21} = G^2_{22} = 0. \tag{4.11}$$

After successfully calculating the coefficients of nonlinear and Berwald connection, our analytical journey leads us to the computation of the coefficients of the deviation curvature tensor equation (2.9). This pivotal step equips us with the tools necessary to make informed assessments about the Jacobi stability of the system.

Henceforth, the deviation curvature tensor, commonly recognized as the second KCC invariant, can be derived as follows:

$$P^1_1 = \tfrac{1}{2}(Y^2) - 1 + \tfrac{1}{4}(X^2)^2 - \tfrac{1}{2}(X^1)^2,$$
$$P^1_2 = \tfrac{1}{2}Y^1 + \tfrac{1}{4}X^1X^2,$$
$$P^2_1 = -Y^1 - \tfrac{1}{2}X^1X^2,$$
$$P^2_2 = -\tfrac{1}{2}(X^1)^2. \tag{4.12}$$

In Figs. 8 and 9, the temporal evolution of P^j_i components is illustrated for identical initial conditions as previously employed in Fig. 7. Specifically, the components of P^j_i delineate the variation for the nested tori when initialized at (0,1,1) and the chaotic sea for the initial condition (0,5,1), respectively.

Specifically the P^i_j matrix is given by $\begin{bmatrix} P^1_1 & P^2_1 \\ P^1_2 & P^2_2 \end{bmatrix}$ and its eigenvalues can be acquired as

$$\lambda_{1,2} = \frac{1}{2}\left[P^1_1 + P^2_2 \pm \sqrt{\left(P^1_1 - P^2_2\right)^2 + 4P^2_1P^1_2}\right], \tag{4.13}$$

which satisfies the characteristics equation

$$\lambda^2 - \left(P^1_1 + P^2_2\right)\lambda + \left(P^1_1P^2_2 - P^1_2P^2_1\right) = 0. \tag{4.14}$$

According to Routh-Hurwitz criteria, the system is Jacobi stable if

$$P^1_1 + P^2_2 < 0, \quad P^1_1P^2_2 - P^1_2P^2_1 > 0, \tag{4.15}$$

otherwise it is Jacobi unstable.

From Eq. (4.13), it becomes evident that the eigenvalues are solely determined by the coordinates (X^1, X^2, Y^1, Y^2). Consequently, this insight provides us with a comprehensive visualization of the basin, particularly within the $(X^1$-$X^2)$ plane, where the eigenvalues can assume positive, negative, or complex values.

Crucially, it is noteworthy that the entire framework of the KCC theory hinges on the dynamics of nearby trajectories around initial points. This sets it apart from conventional linearization methods that necessitate prior knowledge of equilibrium points. Consequently, the KCC theory offers a more robust analytical approach for determining the basin of attraction, even in systems devoid of fixed points, as opposed to the arduous task of numerically evaluating Lyapunov exponents.

We take a significant step forward by proceeding to evaluate the deviation vector ξ^i, a decisive element that provides crucial insights into the onset and characterization of chaos within the system of Eqs. (4.1)–(4.3). One can write the differential equations of ξ^i by Eq. (2.8) as

$$\frac{d^2\xi^1}{dt^2} - X^2\frac{d\xi^1}{dt} - X^1\frac{d\xi^2}{dt} + (1 - Y^2)\xi^1 - Y^1\xi^2 = 0, \tag{4.16}$$

$$\frac{d^2\xi^2}{dt^2} + 2X^1\frac{d\xi^1}{dt} + 2Y^1\xi^1 = 0. \tag{4.17}$$

Then by Eq. (4.6), the above equations can be written as

$$\frac{d^2\xi^1}{dt^2} - z\frac{d\xi^1}{dt} - x\frac{d\xi^2}{dt} + (1 - \dot{z})\xi^1 - \dot{x}\xi^2 = 0, \tag{4.18}$$

$$\frac{d^2\xi^2}{dt^2} + 2x\frac{d\xi^1}{dt} + 2\dot{x}\xi^1 = 0. \tag{4.19}$$

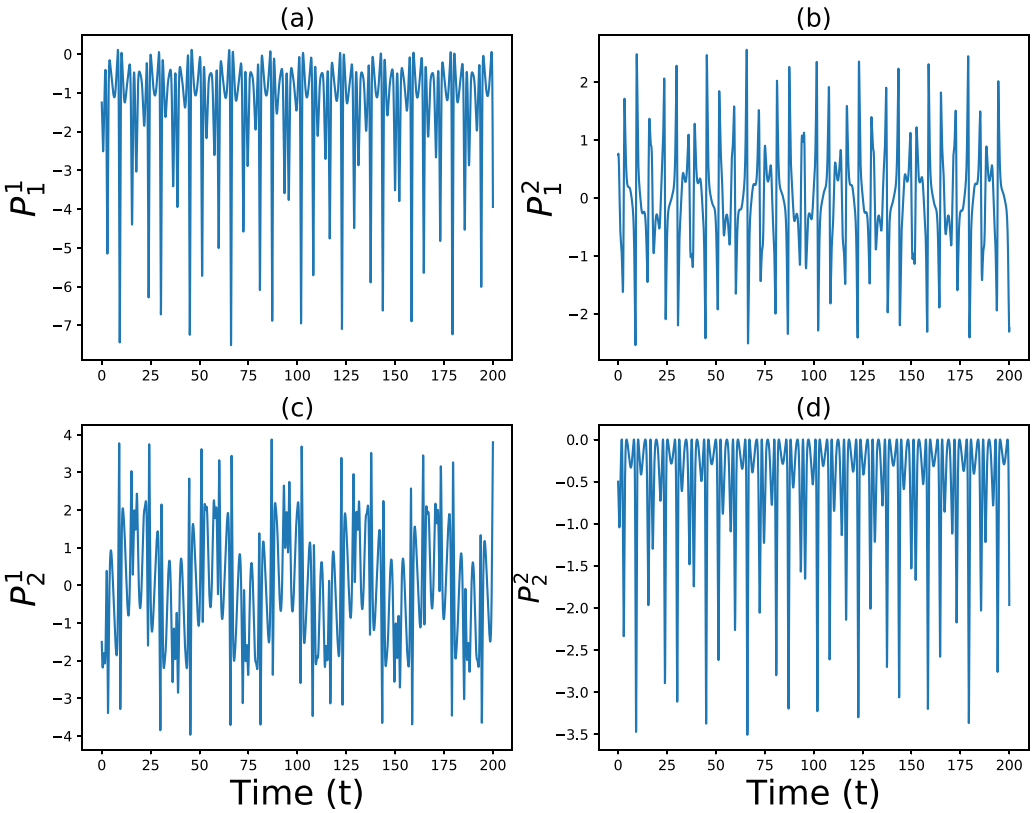

FIG. 8. Components of the deviation curvature tensor P_j^i, Eq. (4.12), of the system of Eqs. (4.1)–(4.3) with the initial condition (0,1,1) forming a nested tori. (a) P_1^1 (t) vs time (t). (b) P_2^1 (t) vs time (t). (c) P_1^2 (t) vs time (t). (d) P_2^2 (t) vs time (t).

Given that the system lacks equilibrium points, describing the behavior of deviation vectors through local stability analysis, as done in the previous case, is not applicable. However, by utilizing Eqs. (4.18) and (4.19), we can numerically compute the instability exponent. This provides a means to characterize the basin of attraction (see Fig. 10) for this type of hidden attractor.

The presented graphical representation offers a compelling insight into the consistency between the numerically computed basin using the maximum Lyapunov exponent and the

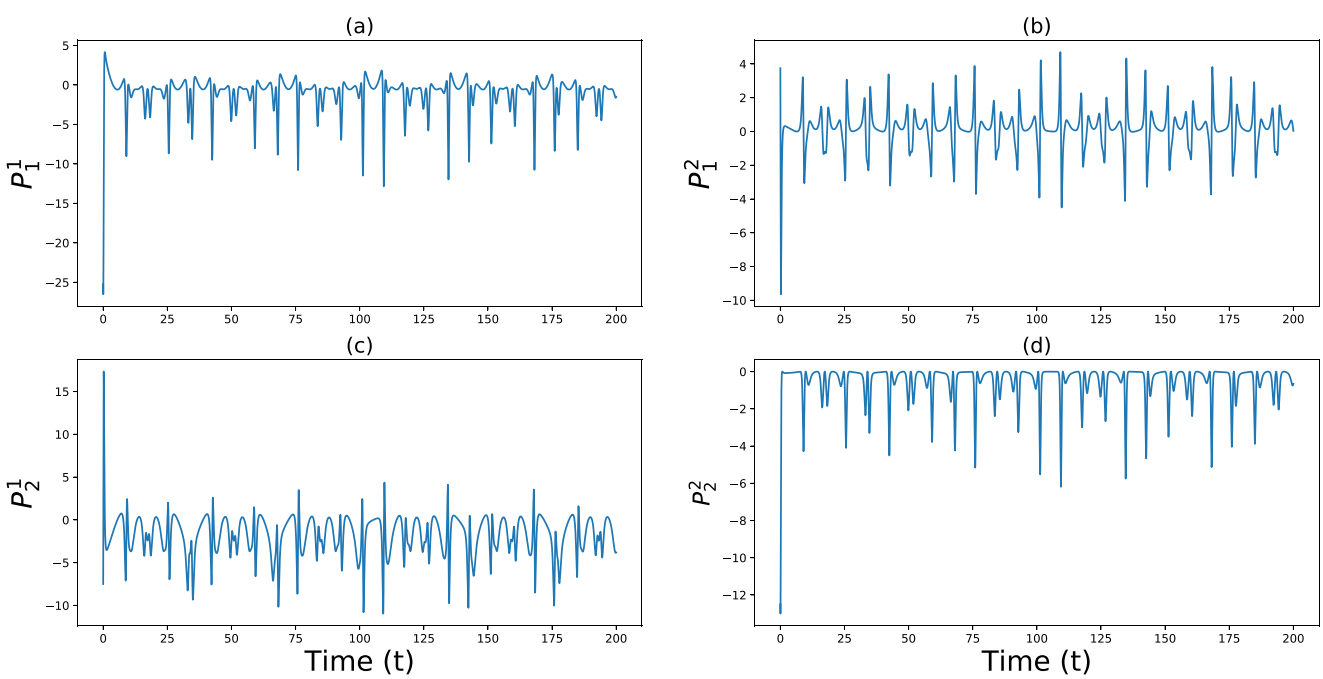

FIG. 9. Components of deviation curvature tensor P_j^i, Eq. (4.12), of the system of Eqs. (4.1)–(4.3) with the initial condition (0,5,1) forming a chaotic attractor. (a) P_1^1 (t) vs time (t). (b) P_2^1 (t) vs time (t). (c) P_1^2 (t) vs time (t). (d) P_2^2 (t) vs time (t).

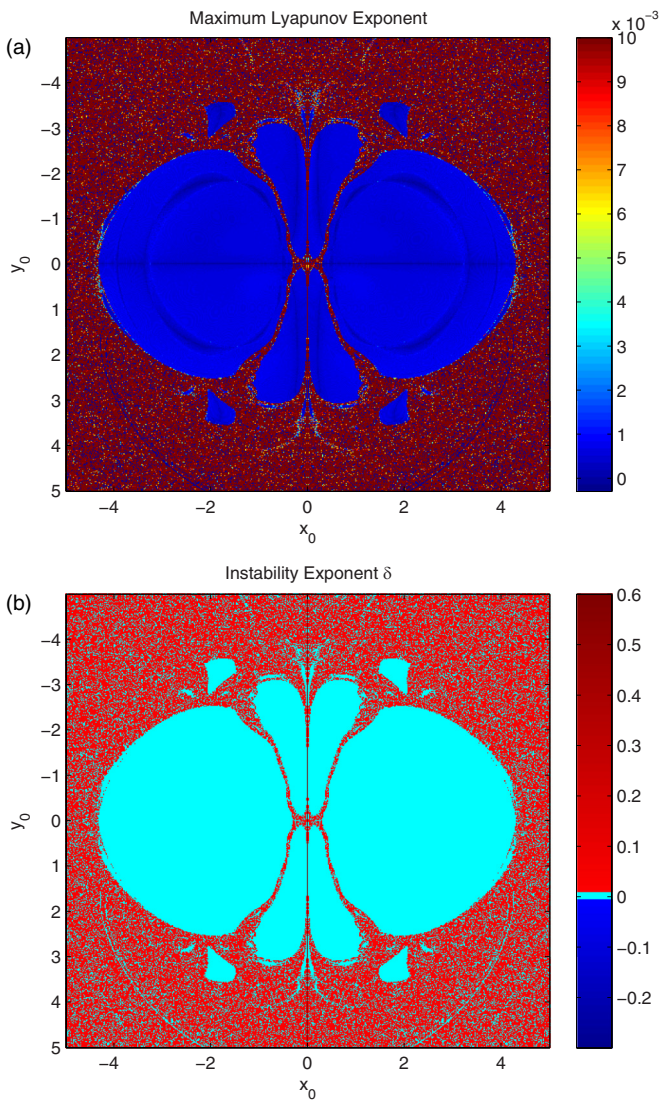

FIG. 10. Basin of attraction of the system of Eqs. (4.1)–(4.3). (a) Basin (x_0, y_0) is numerically determined by the estimation of the maximum Lyapunov exponent. (b) Basin determined by calculating the instability exponent δ with the help of the deviation vector computed from Eqs. (4.18) and (4.19).

basin derived from the instability exponent obtained through the two analytically coupled differential equations. This observation holds true not only for the system with a stable equilibrium but also extends to the system without equilibrium points. The virtually perfect match in both scenarios attests to the robustness and versatility of our analytical approach. It underscores the effectiveness of deriving instability exponents from the coupled differential equations, offering a reliable and comprehensive understanding of the basin of attraction, even in systems lacking equilibrium points.

V. CONCLUSIONS

In conclusion, our exploration has provided profound insights into the intricate dynamics of two distinct autonomous 3D systems. The first system, characterized by a singular stable fixed point, exhibited unexpected chaotic behavior, challenging conventional expectations from linear stability analysis. Utilizing the Kosambi-Cartan-Chern (KCC) theory, we successfully captured the basin of attraction for this system through the analytical depiction of deviation vectors and curvature variation, unveiling hidden chaotic oscillations.

Equally intriguing was the examination of the second system, which lacked equilibrium points altogether. By numerically computing the instability exponent using Eqs. (4.18) and (4.19), we effectively characterized the basin of attraction for this unique hidden attractor. This analytical approach provides a valuable alternative to the conventional numerical evaluation of Lyapunov exponents, demonstrating the robustness and versatility of the KCC theory.

The comprehensive visualization of basins, as demonstrated in Figs. 4 and 5, not only substantiates the efficacy of the instability exponent in predicting chaotic zones but also underscores the superiority of the KCC theory in offering analytical insights into the behavior of complex dynamical systems. This work contributes significantly to the understanding of hidden attractors, showcasing the KCC theory as a powerful tool for capturing nuanced dynamics, even in scenarios where equilibrium points are absent. Indeed, the applicability of this method is not confined solely to autonomous systems but can be extended to nonautonomous systems as well. This extension is facilitated by augmenting the dimension of the system, effectively converting it into an autonomous one. Consequently, the theory can be readily applied to investigate the chaotic behavior of forced duffing, van der Pol, and various other relevant systems. Furthermore, this theoretical framework lends itself to a geometrical interpretation, offering a visual representation that enhances our understanding of the intricate dynamics exhibited by these systems.

ACKNOWLEDGMENT

S.R. expresses gratitude to Dr. Tanmoy Paul for his profound insights and valuable discussions during the course of this work.

[1] Y. Ueda, N. Akamatsu, and C. Hayashi, Computer simulations and non-periodic oscillations, Trans. IEICE Japan **56A**, 218 (1973).

[2] E. N. Lorenz, Deterministic nonperiodic flow, J. Atmos. Sci. **20**, 130 (1963).

[3] U. Feudel, Complex dynamics in multistable systems, Int. J. Bifurcation Chaos **18**, 1607 (2008).

[4] M. D. Shrimali, A. Prasad, R. Ramaswamy, and U. Feudel, The nature of attractor basins in multistable systems, Int. J. Bifurcation Chaos **18**, 1675 (2008).

[5] S. Kraut and U. Feudel, Multistability, noise, and attractor hopping: The crucial role of chaotic saddles, Phys. Rev. E **66**, 015207(R) (2002).

[6] A. N. Pisarchik and U. Feudel, Control of multistability, Phys. Rep. **540**, 167 (2014).

[7] A. Chudzik, P. Perlikowski, A. Stefanski, and T. Kapitaniak, Multistability and rare attractors in van der Pol-Duffing oscillator, Int. J. Bifurcation Chaos **21**, 1907 (2011).

[8] S. L. T. de Souza, A. M. Batista, I. L. Caldas, R. L. Viana, and T. Kapitaniak, Noise-induced basin hopping in a vibro-impact system, Chaos, Solitons Fractals **32**, 758 (2007).

[9] B. Blażejczyk-Okolewska and T. Kapitaniak, Co-existing attractors of impact oscillator, Chaos, Solitons Fractals **9**, 1439 (1998).

[10] B. Blazejczyk-Okolewska and T. Kapitaniak, Dynamics of impact oscillator with dry friction, Chaos, Solitons Fractals **7**, 1455 (1996).

[11] T. Kapitaniak, Generating strange nonchaotic trajectory, Phys. Rev. E **47**, 1408 (1993).

[12] T. Kapitaniak, Stochastic response with bifurcations to nonlinear Duffing's oscillator, J. Sound Vib. **102**, 440 (1985).

[13] A. Silchenko, T. Kapitaniak, and V. S. Anishchenko, Noise-enhanced phase locking in a stochastic bistable system driven by a chaotic signal, Phys. Rev. E **59**, 1593 (1999).

[14] N. V. Kuznetsov, G. A. Leonov, and V. I. Vagaitsev, Analytical-numerical method for attractor localization of generalized Chua's system, IFAC Proc. **4**, 29 (2010) (IFAC-PapersOnline).

[15] G. A. Leonov, N. V. Kuznetsov, and V. I. Vagaitsev, Localization of hidden Chua's attractors, Phys. Lett. A **375**, 2230 (2011).

[16] G. A. Leonov, N. V. Kuznetsov, and V. I. Vagaitsev, Hidden attractor in smooth Chua systems, Phys. D (Amsterdam, Neth.) **241**, 1482 (2012).

[17] G. A. Leonov and N. V. Kuznetsov, Hidden attractors in dynamical systems. From hidden oscillations in Hilbert-Kolmogorov, Aizerman, and Kalman problems to hidden chaotic attractors in Chua circuits, Int. J. Bifurcation Chaos **23**, 1330002 (2013).

[18] S. Brezetskyi, D. Dudkowski, and T. Kapitaniak, Rare and hidden attractors in van der Pol-Duffing oscillators, Eur. Phys. J.: Spec. Top. **224**, 1459 (2015).

[19] G. Leonov, N. Kuznetsov, and T. Mokaev, Homoclinic orbits, and self-excited and hidden attractors in a Lorenz-like system describing convective fluidmotion, Eur. Phys. J.: Spec. Top. **224**, 1421 (2015).

[20] S. Nose, A molecular dynamics method for simulations in the canonical ensemble, Mol. Phys. **52**, 255 (1984).

[21] W. G. Hoover, Canonical dynamics: Equilibrium phase-space distributions, Phys. Rev. A **31**, 1695 (1985).

[22] Z. Wei, Dynamical behaviors of a chaotic system with no equilibria, Phys. Lett. A **376**, 102 (2011).

[23] S. Jafari, J. Sprott, and S. Golpayegani, Elementary quadratic chaotic flows with no equilibria, Phys. Lett. A **377**, 699 (2013).

[24] P. Saha, D. C. Saha, A. Ray *et al.*, Memristive non-linear system and hidden attractor, Eur. Phys. J.: Spec. Top. **224**, 1563 (2015).

[25] X. Wang and G. Chen, A chaotic system with only one stable equilibrium, Commun. Nonlinear Sci. **17**, 1264 (2012).

[26] S. Kingni, S. Jafari, H. Simo, and P. Woafo, Three-dimensional chaotic autonomous system with only one stable equilibrium: Analysis, circuit design, parameter estimation, control, synchronization and its fractional-order form, Eur. Phys. J. Plus **129**, 76 (2014).

[27] G. A. Leonov, V. I. Vagaitsev, and N. V. Kuznetsov, Algorithm for localizing Chua attractors based on the harmonic linearization method, Dokl. Math. D **82**, 663 (2010).

[28] D. Dudkowski *et al.*, Hidden attractors in dynamical systems, Phys. Rep. **637**, 1 (2016).

[29] D. Dudkowski, A. Prasad, and T. Kapitaniak, Perpetual points and hidden attractors in dynamical systems, Phys. Lett. A **379**, 2591 (2015).

[30] D. D. Kosambi, Parallelism and path-spaces, Math. Z. **37**, 608 (1933).

[31] E. Cartan and D. D. Kosambi, Observations sur le mémoire précédent, Math. Z. **37**, 619 (1933).

[32] S. S. Chern, Sur la géométrie d'un systme d'équations différentielles du second ordre, Bull. Sci. Math. **63**, 206 (1939).

[33] P. L. Antonelli, R. S. Ingarden, and M. Matsumoto, *The Theory of Sprays and Finsler Spaces with Applications in Physics and Biology* (Springer, Dordrecht, 1993).

[34] H. Rund, *The Differential Geometry of Finsler Spaces* (Springer, Berlin, 2012).

[35] C. G. Böhmer, T. Harko, and S. V. Sabau, Jacobi stability analysis of dynamical systems—Applications in gravitation and cosmology, Adv. Theor. Math. Phys. **16**, 1145 (2012).

[36] T. Harko, C. Y. Ho, C. S. Leung, and S. Yip, Jacobi stability analysis of the Lorenz system, Int. J. Geom. Methods Mod. Phys. **12**, 1550081 (2015).

[37] Q. Huang, A. Liu, and Y. Liu, Jacobi stability analysis of the Chen system, Int. J. Bifurcation Chaos **29**, 1950139 (2019).

[38] M. K. Gupta and C. K. Yadav, Jacobi stability analysis of Rössler system, Int. J. Bifurcation Chaos **27**, 1750056 (2017).

[39] M. K. Gupta and C. K. Yadav, Jacobi stability analysis of modified Chua circuit system, Int. J. Geom. Methods Mod. Phys. **14**, 1750089 (2017).

[40] M. K. Gupta and C. K. Yadav, Rabinovich–Fabrikant system in view point of KCC theory in Finsler geometry, J. Interdiscip. Math. **22**, 219 (2019).

[41] P. L. Antonelli, S. F. Rutz, and V. S. Sabău, A transient-state analysis of Tyson's model for the cell division cycle by means of KCC-theory, Open Syst. Inf. Dyn. **09**, 223 (2002).

[42] M. K. Gupta and C. K. Yadav, KCC theory and its application in a tumor growth model, Math. Methods Appl. Sci. **40**, 7470 (2017).

[43] F. Munteanu, A study of the Jacobi stability of the Rosenzweig-MacArthur predator-prey system through the KCC geometric theory, Symmetry **14**, 1815 (2022).

[44] K. Yamasaki and T. Yajima, Lotka-Volterra system and KCC theory: Differential geometric structure of competitions and predations, Nonlinear Anal.: Real World Appl. **14**, 1845 (2013).

[45] Y. Liu, C. Li, and A. Liu, Analysis of geometric invariants for three types of bifurcations in 2D differential systems, Int. J. Bifurcation Chaos **31**, 2150105 (2021),

[46] K. Yamasaki and T. Yajima, KCC analysis of the normal form of typical bifurcations in one-dimensional dynamical systems: Geometrical invariants of saddle-node, transcritical, and pitchfork bifurcations, Int. J. Bifurcation Chaos **27**, 1750145 (2017).

[47] S. Jafari, J. C. Sprott, and F. Nazarimehr, Recent new examples of hidden attractors, Eur. Phys. J.: Spec. Top. **224**, 1469 (2015).

[48] H. A. Posch, W. G. Hoover, and F. J. Vesely, Canonical dynamics of the Nosé oscillator: Stability, order, and chaos, Phys. Rev. A **33**, 4253 (1986).

[49] W. G. Hoover and H. A. Posch, Shear viscosity via global control of spatiotemporal chaos in two-dimensional isoenergetic dense fluids, Phys. Rev. E **51**, 273 (1995).